

Short-range Si-Al order in leucite and analcime: Determination of the configurational entropy from ^{27}Al and variable-temperature ^{29}Si NMR spectroscopy of leucite, its Cs- and Rb-exchanged derivatives, and analcime

BRIAN L. PHILLIPS*

Earth Sciences Division, Lawrence Livermore National Laboratory, P.O. Box 808, L-219, Livermore, California 94550, U.S.A.

R. JAMES KIRKPATRICK

Department of Geology, University of Illinois at Urbana-Champaign, Urbana, Illinois 61801, U.S.A.

ABSTRACT

We have examined a natural leucite sample, its Rb- and Cs-exchanged derivatives, and analcime using ^{29}Si and ^{27}Al MAS NMR spectroscopy, with the objective of providing a better understanding of the Si-Al distribution in these phases. Spectra were obtained at temperatures from 25 to 600 °C for leucite and from 25 to 200 °C for the Cs-exchanged leucite through its tetragonal-to-cubic structural phase transition. The ^{29}Si NMR spectrum of cubic Cs-exchanged leucite contains five peaks corresponding to the single tetrahedral site having from 0 to 4 next nearest neighbor Al cations. The populations of the five local Si environments indicate the presence of slight additional short-range Si-Al order beyond that produced by Al-Al avoidance. We present expressions from which the configurational entropy (S_c) due to Si-Al disorder can be calculated from the populations of tetrahedral cation clusters determined from NMR spectra or the assumption of Al-Al avoidance. For cubic leucite, the NMR data indicate that S_c due to Si-Al disorder is $6.6 \pm 0.2 \text{ J}/(\text{mol}\cdot\text{K})$, which is comparable with the value of $6.9 \text{ J}/(\text{mol}\cdot\text{K})$ obtained with the assumption of only Al-Al avoidance. The short-range Si-Al order was also investigated for several samples of the structurally related mineral analcime, which show a wide variation of S_c , from 3.1 to $8.1 \text{ J}/(\text{mol}\cdot\text{K})$. The ^{29}Si NMR spectra of the Rb- and Cs-exchanged leucite resemble closely those of the natural leucite at 300 and 600 °C, respectively. The ^{27}Al chemical shifts for all leucite samples display a linear correlation with the mean bridging-bond angle.

INTRODUCTION

Leucite, KAlSi_2O_6 , comprises an aluminosilicate framework of four-, six-, and eight-membered rings of SiO_4 and AlO_4 tetrahedra that exhibits cubic topological symmetry (space group $Ia3d$). At room temperature, leucite is tetragonal (space group $I4_1/a$; Mazzi et al., 1976), but it becomes metrically cubic near 650 °C through a series of structural phase transitions (e.g., Lange et al., 1986, and references therein). The topology of the leucite framework is compatible with a fully ordered 2:1 Si-Al distribution containing no Al-O-Al linkages (for example, the synthetic leucite analogue $\text{K}_2\text{MgSi}_5\text{O}_{12}$ displays complete Mg-Si order; Kohn et al., 1991), but no fully ordered natural leucite has been reported, and there remain some questions about the state of Si-Al order.

The tetragonal phase of leucite at room temperature contains three inequivalent framework sites (designated T1, T2, and T3), for which no long-range Si-Al order with respect to the site occupancies was detected by XRD

(Mazzi et al., 1976). Boysen (1990) noted that fitting the Si-Al site occupancies improves Rietveld refinements of neutron scattering data, but that the site occupancies and displacement factors are correlated and cannot be determined independently. Previous NMR spectroscopic studies reported some long-range order of Si and Al on the three crystallographic sites of the tetragonal structure. However, distinctly different site occupancies were obtained from interpretations of the ^{29}Si (Murdoch et al., 1988) and ^{27}Al (Phillips et al., 1989) NMR data. Although uncertainties in the analysis of both the ^{29}Si and ^{27}Al NMR spectra make it difficult to determine the site-occupancy factors by these methods, there seems to be general agreement on the magnitude of the long-range order, with each of the three T sites containing between 0.2 and 0.5 Al atoms.

Only one crystallographically inequivalent tetrahedral site exists in the high-temperature, cubic form of leucite, which precludes any long-range Si-Al order (Peacor, 1968). However, the observation in the metrically cubic phase of twin boundaries (Heaney and Veblen, 1990) and X-ray reflections (Palmer et al., 1989; Ito et al., 1991) that violate the apparent cubic symmetry suggests that the high-temperature phase might remain locally tetragonal. The

* Present address: Department of Chemical Engineering and Materials Science, University of California, Davis, California 95616, U.S.A.

Si-Al distribution is one possible source of local order in the metrically cubic phase, and several studies have addressed the possible role of Si-Al order on the phase transitions in leucite (Palmer et al., 1989; Hatch et al., 1990; Heaney and Veblen, 1990). On the basis of lattice-energy calculations, Dove et al. (1993) concluded that the strains associated with the cubic-to-tetragonal transition are not related to the state of Si-Al order and that the transition would occur in fully Si-Al-disordered leucite. A better understanding of the relationships in leucite between the Si-Al order, the structural phase transitions, and the true symmetry of the high-temperature phase requires a more thorough characterization of its Si-Al distribution than is currently available.

From a thermochemical standpoint, the energetically significant effects of the Si-Al distribution can be related to the degree of short-range order. For the present study, we describe the state of short-range order in terms of population distributions of small clusters of tetrahedral cations. From ^{29}Si MAS NMR spectra one can obtain information on the populations of clusters ranging in size from cation pairs (e.g., Si-O-Si, Si-O-Al, Al-O-Al) up to the five-membered clusters designated in the Q notation as $Q^n(n\text{Al})$, where Q denotes ^{29}Si , the superscript the number of bridging O atoms, and n the number of next nearest neighbor (NNN) Al atoms ($0 \leq n \leq 4$). Much of the decrease in configurational entropy relative to a purely random Si-Al distribution can be obtained from the distribution of these small clusters, owing to the rapid decrease of the combinatorial with the increase in cluster size. In contrast, site-mixing models that ignore short-range correlations can significantly overestimate the configurational entropy (McConnell, 1985).

The purpose of this study is to determine the state of short-range Si-Al order in the aluminosilicate framework of leucite. Experimentally, this measurement is easiest to make for the cubic phase, without the spectral complications caused by the tetragonal structural distortion. That the cubic and tetragonal phases have the same state of short-range Si-Al order can be expected on the basis of the greatly different time scales for Si-Al diffusion and the reversible cubic-to-tetragonal phase transition. The cubic phase of leucite occurs at temperatures just beyond the reach of current commercial MAS NMR instrumentation, but the substitution of larger alkali cations for K lowers the transition temperature while leaving the framework essentially intact (Taylor and Henderson, 1968). Cs-exchanged leucite is cubic above 97 °C (Palmer et al., in preparation), which is well within the reach of our MAS NMR probes.

Below, we present ^{29}Si and ^{27}Al MAS NMR data for leucite and its Rb- and Cs-exchanged derivatives at room temperature (RT), as well as for leucite from RT to 600 °C and the Cs-exchanged sample from RT to 150 °C. The ^{29}Si spectrum of cubic $\text{CsAlSi}_2\text{O}_6$ contains five peaks corresponding to a single crystallographic site with local configurations $Q^4(4\text{Al})$ to $Q^4(0\text{Al})$. The relative populations of these Si environments indicate only a small degree of

short-range order beyond Al-Al avoidance. However, the configurational entropy for this Si-Al distribution, 6.6 J/(mol·K), is less than half that computed only from the long-range site occupancies obtained from earlier studies. For comparison, we also present data for several samples of the structurally similar mineral analcime that show large variations in the state of order for this phase.

EXPERIMENTAL METHODS

Samples

The leucite used for this study is L999 from the Harker Collection of the University of Cambridge and was described more fully by Palmer et al. (1988). Cs- and Rb-exchanged derivatives (nominally, $\text{CsAlSi}_2\text{O}_6$ and $\text{RbAlSi}_2\text{O}_6$) were prepared by ion exchange of the leucite in molten bromide salt at 1073 K for 3 d. Details of the cation exchange process and compositional and neutron powder-diffraction data are presented in Palmer et al. (in preparation).

Results were also reported for several analcime samples that span a range of composition with respect to Si/Al. The first analcime sample is from Mont Saint Hilaire, Quebec. The second sample was taken from a trapezoidal crystal about 2 cm in diameter, labeled no. 1904 from the University of Illinois mineralogical collection, but of unknown origin. Two fine-grained authigenic analcime samples were examined, one from Barstow, California, and the other from Mojave County, Arizona. All samples appeared to be monomineralic by powder XRD except for some quartz detected in the Barstow sample, which is also evident in the NMR spectra.

NMR spectroscopy

The ^{29}Si MAS NMR spectra of leucite were collected at $H_0 = 8.45$ T (71.5 MHz) with a homemade spectrometer based on a Nicolet 1280 computer and a 290B pulse programmer. For all the spectra at RT , and for those of the Cs-exchanged leucite from RT to 200 °C, we used a Doty Scientific MAS probe, with the sample contained in a 7-mm sapphire rotor spinning at 3–4 kHz. Variable-temperature (VT) spectra for leucite from RT to 600 °C were taken using a Doty Scientific high-temperature MAS probe. The spinning rate in the high-temperature probe was 3 kHz at RT but decreased to about 1.2 kHz at 600 °C. The ^{29}Si NMR spectra at RT were taken with 45° pulse lengths and a 5-s recycle delay. The ^{29}Si spin-lattice relaxation time (T_1) was <2 s for all the leucite samples. Spectra collected for varying recycle delay showed no change in the relative intensities, but a symmetrical broadening was noted for spectra obtained with recycle delays less than about 1 s.

The ^{27}Al MAS NMR data were obtained at $H_0 = 11.7$ T (130.3 MHz) with a spectrometer similar to the one described above using a Doty 5-mm MAS probe and samples spinning at 8 kHz in zirconia rotors. The spectra were obtained using a 1- μs pulse length (the nonselective 90° pulse was 12 μs) and 0.5-s recycle delay, but no change

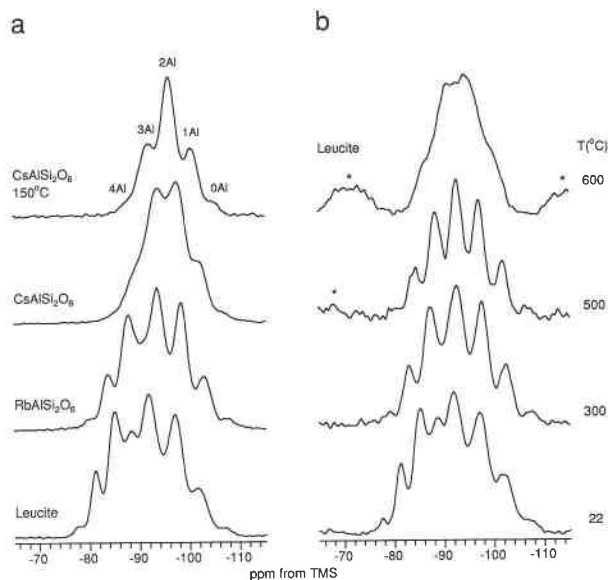


Fig. 1. The ^{29}Si MAS NMR spectra at 71.5 MHz of (a) leucite and its Rb- and Cs-exchanged derivatives and (b) leucite with increasing temperature. Asterisks denote spinning side bands.

in the central transition envelope was observed by varying the pulse length from 1 to 5 μs and the recycle delay from 0.5 to 5 s.

The analcime ^{29}Si NMR spectra were obtained at 59.6 MHz with a Chemagnetics CMX 300 spectrometer and a 7-mm pencil probe. The sample spinning rate was 4–5 kHz. The 90° pulse width was 6 μs , and pulses of 3–6 μs were used to collect the data. The recycle delay varied from 15 to 2000 s, depending on the sample T_1 , which varied from 5 s for the Mojave sample to >1000 s for the UIUC 1904 sample. Total accumulation time for each spectrum was from 0.5 to 4 d. For each sample, we collected several spectra, which differed by the recycle delay used. We found no significant change in the peak intensities with recycle delay except for the Barstow sample, which showed an increase in the intensity of the quartz peak with increasing recycle delay.

The ^{29}Si chemical shifts were referenced to an external sample of tetramethylsilane, and the ^{27}Al shifts were referenced to an external 1-*M* AlCl_3 solution.

RESULTS

The ^{29}Si MAS NMR spectra at *RT* for the series leucite, $\text{RbAlSi}_2\text{O}_6$, and $\text{CsAlSi}_2\text{O}_6$ (Fig. 1a) show a continuous variation caused by changes in the overlap of sets of peaks arising from the three crystallographic sites, as discussed for leucite by Murdoch et al. (1988). For each crystallographic site, there are five peaks corresponding to the local Si environments $Q^4(4\text{Al})$ to $Q^4(0\text{Al})$. The spectrum of the leucite sample is nearly identical to those presented by Murdoch et al. (1988) and Phillips et al. (1989).

For the Cs-exchanged leucite above the tetragonal-to-cubic transition, which occurs at $T_c = 97^\circ\text{C}$ (Palmer et

TABLE 1. Results of the least-squares fit of the ^{29}Si NMR spectrum of Cs-exchanged leucite at 150°C

Si environment	δ (ppm)	FWHM (ppm)	Relative intensity	Calculated intensity (Al-Al avoidance)
4Al	-87.1(2)	3.7(3)	0.037(5)	0.070
3Al	-91.7(1)	4.3(1)	0.277(6)	0.264
2Al	-96.0	3.3	0.427(5)	0.374
1Al	-100.4	3.5	0.221(1)	0.236
0Al	-104.8	3.0	0.038(1)	0.056

Note: numbers in parentheses refer to estimated uncertainty; otherwise uncertainty is less than one unit in the last digit. Calculated intensities are with the assumption of a random Si-Al distribution after the exclusion of Al-O-Al linkages.

al., in preparation), the ^{29}Si NMR spectrum consists of five well-resolved peaks due to the single crystallographic site having from 4 to 0 Al NNN (left to right in the spectrum of Fig. 1). Additional peaks in the *RT* spectrum of $\text{CsAlSi}_2\text{O}_6$ support the conclusion of Palmer et al. (in preparation) that the Cs-exchanged leucite is tetragonal at *RT* (cf. Taylor and Henderson, 1968). The results of least-squares fits of the spectrum of cubic $\text{CsAlSi}_2\text{O}_6$ to a sum of Gaussian curves are presented in Table 1. The value of Si/Al computed from the intensities of the ^{29}Si NMR peaks with the assumption of no Al-O-Al linkages

$$\text{Si/Al} = 4 \left/ \sum_{n=1}^4 n \cdot I_{Q^4(n\text{Al})} \right. \quad (1)$$

(Corbin et al., 1987) is 1.95 ± 0.05 and agrees well with that obtained by electron microprobe: 1.99 ± 0.10 (Palmer et al., in preparation). Spectra for $\text{CsAlSi}_2\text{O}_6$ were taken at 25, 100, 120, 150, and 200 $^\circ\text{C}$. The changes in the spectrum from 25 to 150 $^\circ\text{C}$ are continuous, but we observed no significant difference between the spectra taken at 150 and 200 $^\circ\text{C}$.

The changes in the ^{29}Si NMR spectrum of leucite with increasing temperature (Fig. 1b) parallel those that occur with increasing size of the alkali cation. Specifically, the spectra of the parent leucite at 300 and 600 $^\circ\text{C}$ are very similar to those of the Rb- and Cs-exchanged leucite at *RT*, respectively (cf. Fig. 1). The spectrum of leucite is best resolved near 500 $^\circ\text{C}$, which probably indicates that near this temperature the chemical-shift difference between the crystallographic sites is about the same as the separation between the $Q^4(n\text{Al})$ and $Q^4[(n+1)\text{Al}]$ peaks. The peak separations at 500 $^\circ\text{C}$ are from 4.2 to 4.8 ppm, and the separations between the $Q^4(n\text{Al})$ peaks for cubic $\text{CsAlSi}_2\text{O}_6$ are 4.4 ± 0.2 ppm.

The ^{29}Si MAS NMR spectra of analcime show systematic changes consistent with the values of Si/Al (Fig. 2). The spectrum of sample UIUC 1904 is very similar to that presented by Murdoch et al. (1988). With increasing Si content, the intensity of peaks corresponding to Si-rich local configurations increases [e.g., $Q^4(1\text{Al})$ and $Q^4(0\text{Al})$ at -102 and -107.5 ppm, respectively]. We obtained relative intensities from least-squares fits of the spectra

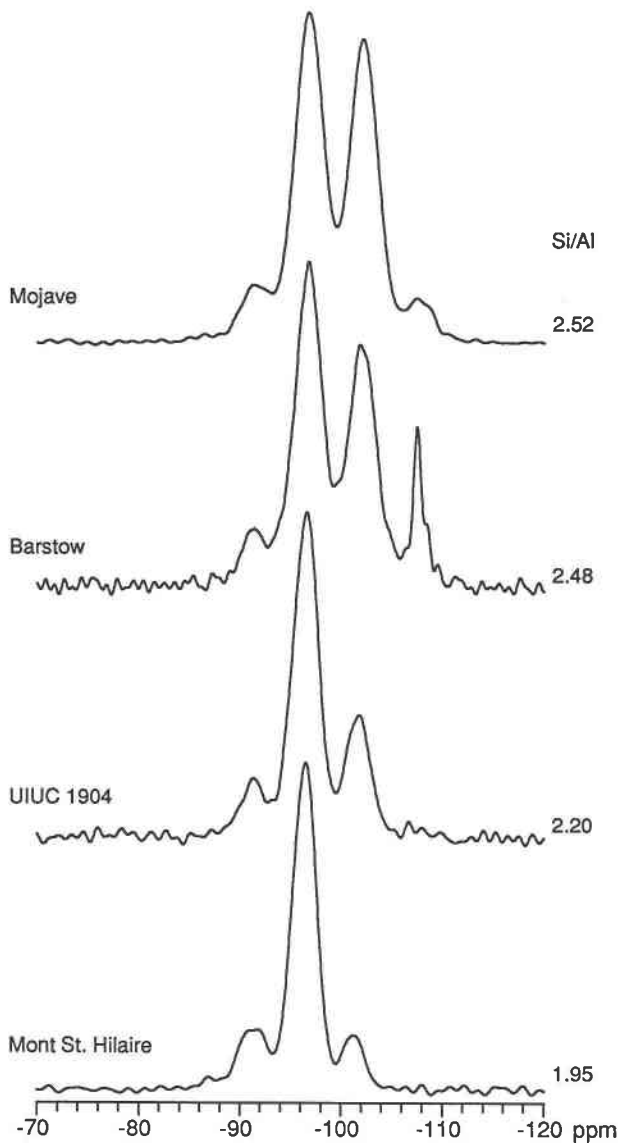


Fig. 2. The ^{29}Si MAS NMR spectra of various analcime samples studied. The Si-Al ratios listed to the right of the spectra were calculated from the peak intensities using Eq. 1. From top to bottom: Mojave County, Arizona, recycle delay 15 s, 4320 acquisitions; Barstow, California, recycle delay 300 s, 240 acquisitions; UIUC 1904 (locality unknown), recycle delay 2000 s, 80 acquisitions; Mont Saint Hilaire, recycle delay 1200 s, 288 acquisitions. No line broadening has been applied to the spectra.

to a sum of Gaussian curves (Table 2). For each sample, the spectra obtained with different recycle delays gave best-fit relative intensities that were constant within $\pm 1\%$ (absolute). Fits to the spectra of the Barstow sample included an additional, narrow peak for the quartz component, the intensity of which increased with recycle delay, although the distribution of the remaining intensity among the analcime peaks did not change appreciably. All the fitted peak positions are in good agreement with the results of Murdoch et al. (1988).

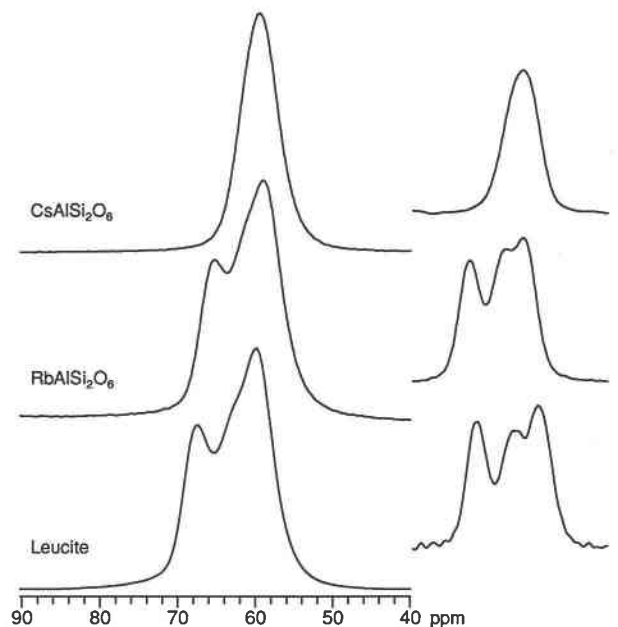


Fig. 3. The ^{27}Al MAS NMR spectra of leucite and its Rb- and Cs-exchanged derivatives taken at 130.3 MHz. (left) Central transition and (right) one of the spinning side bands of the $\pm(\frac{3}{2}, \frac{1}{2})$ satellite transitions at the same horizontal scale and $20\times$ vertical scale.

The ^{27}Al NMR spectrum of the Rb-exchanged leucite (Fig. 3) is similar to that reported previously for leucite (Phillips et al., 1989) but is slightly less resolved. Fitting this spectrum with Voigt line shapes gives peak intensities the same within experimental error as those presented by Phillips et al. (1989) for the parent leucite sample (also shown in Fig. 3). The Cs-exchanged leucite gives a single ^{27}Al MAS NMR peak with a full-width at half-height (FWHH) of 5.6 ppm, although, on the basis of the difference of average T-O-T angles from the crystal-structure refinement of this sample and the line widths of the peaks for the K and Rb forms, we expected to resolve separate peaks for T3 and T1 + T2.

For the Rb-exchanged leucite, the $\pm(\frac{3}{2}, \frac{1}{2})$ satellite-transition spinning sidebands exhibited better resolution than the center band, which allowed a third peak to be clearly distinguished, as was noted previously for leucite (Phillips et al., 1989). However, the satellite spinning sidebands for $\text{CsAlSi}_2\text{O}_6$ showed only a slight narrowing with respect to the center band (from 5.6 to 5.2 ppm, FWHH). This result may indicate greater dispersion of chemical shifts or quadrupolar coupling constants for the Cs-exchanged leucite than for the Rb-exchanged and parent leucite samples.

The isotropic chemical shifts for all resolved peaks (Table 3) were obtained from the center of gravity of the satellite transitions as described by Phillips et al. (1989). These chemical shifts correlate linearly with the mean intertetrahedral angle per T site ($\langle\theta\rangle$; Fig. 4), giving a slope very similar to those presented by Lippmaa et al. (1986) and Phillips et al. (1989):

TABLE 2. Best-fit intensities of ^{29}Si NMR peaks for analcime samples studied

Sample	Peak intensity					Si/Al (± 0.05)
	4Al	3Al	2Al	1Al	0Al	
Mont Saint Hilaire	0.016	0.157	0.695	0.122	0.010	1.95
UIUC 1904	n.d.	0.119	0.619	0.239	0.023	2.18
Barstow	0.005	0.090	0.463	0.365	0.077	2.53
Mojave	0.008	0.087	0.446	0.402	0.058	2.52

Note: n.d. means none detected. Estimated uncertainties for the peak intensities are ± 0.005 absolute, except where noted.

$$\delta_i = 138.8 - 0.538\langle\theta\rangle, \quad r^2 = 0.98. \quad (2)$$

The values of $\langle\theta\rangle$ were obtained from structure refinements of powder neutron diffraction data for a similar set of samples (Palmer et al., in preparation). For the Cs-exchanged leucite, we used the average of the three crystallographic sites because only one peak was observed. Although the correlation expressed in Equation 1 is useful for assigning the NMR peaks, we note that the intertetrahedral angles are averages over both the Si and Al atoms that occupy a given T site. Therefore, the correlation expressed in Equation 2 may not hold for other systems.

The relative shift of the central transition and $\pm(3/2, 1/2)$ satellite-transition centers of gravity is 1.1 ± 0.1 ppm for both $\text{RbAlSi}_2\text{O}_6$ and $\text{CsAlSi}_2\text{O}_6$, giving a quadrupolar coupling constant of 1.5 ± 0.2 MHz (Samoson, 1985). These values are slightly smaller than those for leucite: 1.2 ± 0.1 ppm and 1.7 ± 0.2 MHz (Phillips et al., 1989).

DISCUSSION

Comparison of the intensities of the ^{29}Si NMR peaks of the cubic Cs-exchanged leucite with the populations computed for a Si-Al distribution that is random after the exclusion of Al-O-Al linkages (Table 1) shows that the leucite framework contains a slight degree of short-range order beyond Al-Al avoidance. The similarity of the Si-Al ratios determined by NMR and electron microscope and the presence of only one peak in the ^{27}Al NMR spectrum indicate that there is no detectable population of Al-O-Al linkages in this leucite sample. These results for the Cs-exchanged leucite can be taken as general for leucite because the relatively low temperatures and short times required for the alkali exchange should not significantly affect the distribution of Si and Al atoms. Furthermore, no changes in the NMR spectra have been observed after prolonged heating at 1400 °C (Murdoch et al., 1988; Phillips et al., 1989), which would seem to indicate that even this degree of heat treatment does not affect the average Si-Al distribution of leucite.

The principal difference between the observed Si-Al distribution and one that is random after excluding Al-O-Al linkages is that the observed distribution contains more $Q^4(2\text{Al})$ and correspondingly fewer $Q^4(4\text{Al})$ and $Q^4(0\text{Al})$. This short-range ordering pattern corresponds to a partial decrease of the number of Al-O-Si-O-Al and

TABLE 3. The ^{27}Al chemical-shift data for the leucite samples studied

Sample	Site	$\langle\angle\text{T-O-T}\rangle$ (°)	δ_i (ppm)
Leucite	T1	145.3	61.0
	T2	138.4	64.7
	T3	129.7	69.2
$\text{RbAlSi}_2\text{O}_6$	T1	147.5	59.7
	T2	141.4	62.8
	T3	133.0	67.0
$\text{CsAlSi}_2\text{O}_6$	T1	147.7	60.5*
	T2	144.8	60.5*
	T3	139.4	60.5*

Note: bond angles from Palmer et al. (in preparation); ^{27}Al chemical shifts were determined from the $\pm(3/2, 1/2)$ satellite-transition spinning side bands. * Only one peak was detected for $\text{CsAlSi}_2\text{O}_6$.

Si-O-Si-O-Si linkages in favor of Si-O-Si-O-Al linkages (e.g., Dempsey's rule: Dempsey et al., 1969). A similar short-range ordering pattern has been observed in layer silicates (Herrero and Sanz, 1991) and in synthetic faujasite-type zeolites (Herrero, 1991), for which the driving force for Si-Al order beyond Al-Al avoidance was determined to be a homogeneous distribution of Al-atoms rather than minimization of the number of Al-O-Si-O-Al linkages (Herrero and Sanz, 1991).

For leucite, the Si-Al order indicated by the populations of the $Q^4(n\text{Al})$ tetrahedral cation clusters (pentads) corresponds to only a small decrease of configurational entropy relative to a distribution governed only by Al-Al avoidance. An estimate of the configurational entropy attributed to Si-Al disorder can be obtained from the ^{29}Si NMR results by adapting an algorithm for the cluster-variation technique described by de Fontaine (1979). For any tetrahedral aluminosilicate framework, the logarithm of the number of Si-Al configurations (Ω), including correlations up to those that affect the pentad populations, is given by

$$\ln \Omega = - \sum_i d_{p,i} x_{p,i} \ln x_{p,i} + 2 \sum_j d_{d,j} x_{d,j} \ln x_{d,j} \quad (3)$$

where i spans the six possible pentad configurations [Si(4Al), Si(3Al), \dots Si(0Al), Al(4Si)] having probability x and degeneracy $d(\Sigma_i d_{p,i} = 1)$, and similarly, j covers the possible dyads (pairs) Si-Si, Si-Al, and Al-Al ($x_{\text{Al-Al}}$ is assumed to be 0). From the intensities of the ^{29}Si NMR peaks given in Table 1, the configurational entropy per mole $[\text{AlSi}_2\text{O}_6]^-$, $S_c = 3R \ln \Omega$, is 6.6 J/(mol·K) (Table 4).

For comparison, a similar technique can be applied to calculate the number of Si-Al configurations considering only pairwise correlations:

$$\ln \Omega = -2 \sum_j d_{d,j} x_{d,j} \ln x_{d,j} + 3[x_{\text{Si}} \ln x_{\text{Si}} + x_{\text{Al}} \ln x_{\text{Al}}] \quad (4)$$

where j spans the possible dyads as for Equation 3, and x_{Si} and x_{Al} are, respectively, the fraction of Si and Al. Provided Al-Al avoidance can be assumed ($x_{\text{Al-Al}} = 0$) and there is only one crystallographic site (or all crystallographic sites have the same Si-Al occupancy), then $x_{\text{Si-Al}}$

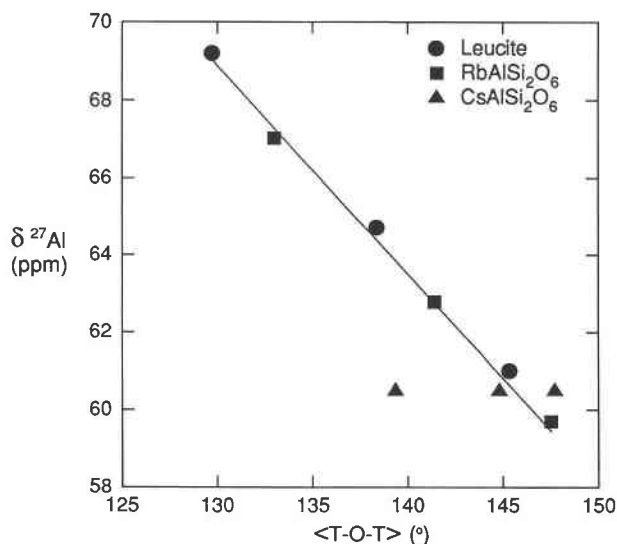


Fig. 4. Variation of ^{27}Al isotropic chemical shifts at room temperature for leucite and its Rb- and Cs-exchanged derivatives with average bridging bond angle (Palmer et al., in preparation). Line is a linear least-squares fit, including the average for the three sites of $\text{CsAlSi}_2\text{O}_6$ (only one peak is observed).

$= x_{\text{Al}}$ and $x_{\text{Si-Si}} = 1 - 2x_{\text{Al}}$, which reduces Equation 4 to

$$\ln \Omega = 3(1 - x_{\text{Al}})\ln(1 - x_{\text{Al}}) - x_{\text{Al}}\ln x_{\text{Al}} - 2(1 - 2x_{\text{Al}})\ln(1 - 2x_{\text{Al}}). \quad (5)$$

This result can be applied generally to framework aluminosilicates to compute the maximum value for the configurational entropy consistent with Al-Al avoidance. For example, Equation 5 gives an improved estimate for S_c of high albite [13.1 J/(mol·K)] that is slightly higher than the value of 12.2 J/(mol·K) estimated by Kerrick and Darken (1975) and significantly lower than that for complete Si-Al disorder [18.7 J/(mol·K)].

Application of Equation 5 to the present leucite samples gives a configurational entropy of 6.9 J/(mol·K), which differs from that computed from Equation 3 by only 0.3 J/(mol·K). That the values obtained from Equations 3 and 5 are similar indicates that the entropy decrease attributed to correlations extending beyond two neighboring tetrahedral cations (e.g., Dempsey's rule) is not energetically significant for leucite and that good approximations for S_c can be obtained simply from Equation 5.

The value of S_c we obtained for leucite, 6.6 J/(mol·K), is significantly lower than those obtained by assuming a purely random Si-Al distribution and simple mixing models based on the long-range ordering patterns proposed by other NMR studies. Commonly accepted values for the standard entropy of leucite (e.g., Robie et al., 1978) contain no zero-point entropy, whereas Ulbrich and Waldbaum (1976) proposed a value of 15.9 J/(mol·K), corresponding to a fully disordered aluminosilicate framework. Our data indicate that the zero-point entropy

TABLE 4. Configurational entropy attributed to Si-Al disorder at various levels of approximation for leucite and analcime samples studied

Sample	Si/Al	S_c [J/(mol·K)]		
		Random	Al-Al avoidance	NMR
L999	Leucite	16.0	6.9	6.6
	Analcime			
Murdoch et al. (1988)	2.13	15.6	7.9	5.2
Mont Saint Hilaire	1.95	16.0	6.9	3.1
UIUC 1904	2.18	15.5	8.1	5.1
Barstow	2.53	14.9	9.1	8.1
Mojave	2.52	14.9	9.1	7.9

Note: estimated uncertainties are ± 0.05 for the Si-Al ratios and ± 0.2 for S_c . Si-Al ratios were computed from Eq. 1, and entropy values for the last two columns were calculated from Eqs. 5 and 3, respectively.

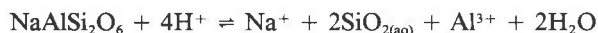
is about 6.6 J/(mol·K). Previous NMR studies (Murdoch et al., 1988; Phillips et al., 1989) reported some long-range order on the three crystallographic sites of tetragonal leucite. Although the site occupancies proposed by these studies differ significantly from each other, each gives a value of about 15.0 ± 0.2 J/(mol·K) for S_c in a simple mixing model, which is only slightly smaller than the value for complete disorder. However, combination of the site-occupancy factors proposed by these studies with a short-range distribution that is random after exclusion of Al-O-Al linkages gives S_c values in good agreement with that for cubic leucite: 6.8 J/(mol·K) for the site occupancies given by Murdoch et al. (1988) and 6.6 J/(mol·K) for those of Phillips et al. (1989). This result suggests that there may be a close relationship between the site-occupancy factors of tetragonal leucite and the short-range Si-Al order beyond Al-Al avoidance in cubic leucite.

A broad range of site occupancies for tetragonal leucite, including those of the aforementioned studies, are consistent with the average short-range Si-Al distribution in cubic leucite (Table 1). In this sense, the results of the present study do not provide a test of the accuracy of the proposed long-range ordering patterns. In addition, the value for the Si-Al configurational entropy reported here is not likely to be changed significantly by further refinement of the site-occupancy factors, as suggested by the small entropy decrease upon the inclusion of correlations beyond tetrahedral cation pairs [0.3 J/(mol·K) from Eqs. 3–5] and the relatively minor amount of long-range order indicated by the proposed site-occupancy factors.

Equations 3–5 can be applied directly to other framework aluminosilicates such as analcime, which has the same framework topology as leucite but is usually metrically cubic at RT (although, see Mazzi and Galli, 1978). The results for the spectra presented here and the data given by Murdoch et al. (1988) indicate that natural analcime exhibits a wide variation in the state of Si-Al order (Table 4), amounting to differences in S_c of up to 5 J/(mol·K). A close relationship appears to exist between the Si-

Al order and the composition, as indicated by the general trend of increasing value of S_c with Si-Al ratio, from 3.1 J/(mol·K) for the Mont Saint Hilaire sample (Si/Al = 1.95) to ca. 8 J/(mol·K) for the authigenic samples (Si/Al = 2.5). This relationship between S_c and composition arises from a nearly constant fractional decrease in the number of Al-O-Si-O-Al and Si-O-Si-O-Si linkages (and corresponding increase of Si-O-Si-O-Al) relative to that for a Si-Al distribution, which is random except for Al-Al avoidance. These analcime samples contain between 19 and 22.5% fewer Al-O-Si-O-Al linkages than would occur for a random distribution (containing no Al-O-Al linkages), compared with a 7% decrease for leucite. In absolute terms, the decrease of S_c relative to that due only to Al-Al avoidance varies from about 1 J/(mol·K) for the authigenic samples to 3.8 J/(mol·K) for the Mont Saint Hilaire sample.

These results suggest that thermochemical calculations for reactions involving analcime may contain a large uncertainty caused by the variability of the configurational entropy term. For example, the addition of a zero-point configurational entropy of 8 J/(mol·K) for analcime increases the solubility product of the reaction



by about 0.5 log units at 25 °C. The present results indicate that using only Al-Al avoidance (Eq. 5) gives too large a value for the configurational entropy of analcime. However, the trend of S_c with composition suggests that, with additional study on more and better characterized analcime samples, a general model may be developed for determining the configurational contribution to the entropy from the composition. Further work is also needed to determine the relative importance of thermochemical and kinetic factors governing the degree of short-range Si-Al order and its effect on the stability field of analcime (e.g., Johnson et al., 1982). The results of the present study, however, indicate that much information on the Si-Al distribution and improved estimates for S_c can be obtained from ^{29}Si MAS NMR data.

ACKNOWLEDGMENTS

We wish to thank David Palmer for providing the Rb- and Cs-exchanged leucite samples and the results of crystal structure refinements prior to publication. We are grateful to William Bourcier for helpful discussion of thermochemical calculations and to Ray Dupree and an anonymous reviewer for helpful critical comments. The research was supported in part by NSF grant EAR-9004260 to R.J.K.

REFERENCES CITED

- Boysen, H. (1990) Neutron scattering and phase transitions in leucite. In E.K.H. Salje, Ed., *Phase transitions in ferroelastic and co-elastic crystals*, p. 334–349. Cambridge University Press, Cambridge, U.K.
- Corbin, D.R., Burgess, B.F., Jr., Vega, A.J., and Farlee, R.D. (1987) Comparison of analytical techniques for the determination of silicon and aluminum content in zeolites. *Analytical Chemistry*, 59, 2722–2728.
- de Fontaine, D. (1979) Configurational thermodynamics of solid solutions. *Solid State Physics*, 34, 73–273.
- Dempsey, E., Kühl, G.H., and Olson, D.H. (1969) Variation of the lattice parameter with aluminum content in synthetic sodium faujasites: Evidence for ordering of the framework ions. *Journal of Physical Chemistry*, 73, 387–390.
- Dove, M.T., Cool, T., Palmer, D.C., Putnis, A., Salje, E.K.H., and Winkler, B. (1993) On the role of Al-Si ordering in the cubic-tetragonal phase transition of leucite. *American Mineralogist*, 78, 486–492.
- Hatch, D.M., Ghose, S., and Stokes, H.T. (1990) Phase transitions in leucite, KAlSi_2O_6 : I. Symmetry analysis with order parameter treatment and the resulting microscopic distortions. *Physics and Chemistry of Minerals*, 17, 220–227.
- Heaney, P.J., and Veblen, D.R. (1990) A high-temperature study of the low-high leucite phase transition using the transmission electron microscope. *American Mineralogist*, 75, 464–476.
- Herrero, C.P. (1991) Short-range order of the Si,Al distribution on the faujasite framework. *Journal of Physical Chemistry*, 95, 3282–3288.
- Herrero, C.P., and Sanz, J. (1991) Short-range order of the Si,Al distribution in layer silicates. *Journal of Physics and Chemistry of Solids*, 52, 1129–1135.
- Ito, Y., Kuehner, S., and Ghose, S. (1991) Phase transitions in leucite determined by high temperature, single crystal X-ray diffraction. *Zeitschrift für Kristallographie*, 197, 75–84.
- Johnson, G.K., Flotow, H.E., O'Hare, P.A.G., and Wise, W.S. (1982) Thermodynamic studies of zeolites: Analcime and dehydrated analcime. *American Mineralogist*, 67, 736–748.
- Kerrick, D.M., and Darken, L.S. (1975) Statistical thermodynamic models for ideal oxide and silicate solid solutions, with application to plagioclase. *Geochimica et Cosmochimica Acta*, 39, 1431–1442.
- Kohn, S.C., Dupree, R., Mortuza, M.G., and Henderson, C.M.B. (1991) An NMR study of structure and ordering in synthetic $\text{K}_2\text{MgSi}_2\text{O}_7$, a leucite analogue. *Physics and Chemistry of Minerals*, 18, 144–152.
- Lange, R.A., Carmichael, I.S.E., and Stebbins, J.F. (1986) Phase transitions in leucite (KAlSi_2O_6), orthorhombic KAlSiO_4 , and their iron analogues (KFeSi_2O_6 , KFeSiO_4). *American Mineralogist*, 71, 937–945.
- Lippmaa, E., Samoson, A., and Mägi, M. (1986) High-resolution ^{29}Al NMR of aluminosilicates. *Journal of the American Chemical Society*, 108, 1730–1735.
- Mazzi, F., and Galli, E. (1978) Is each analcime different? *American Mineralogist*, 63, 448–460.
- Mazzi, F., Galli, E., and Gottardi, G. (1976) The crystal structure of tetragonal leucite. *American Mineralogist*, 61, 108–115.
- McConnell, J.D.C. (1985) Symmetry aspects of order-disorder and the application of Landau theory. *Mineralogical Society of America Reviews in Mineralogy*, 14, 165–186.
- Murdoch, J.B., Stebbins, J.F., Carmichael, I.S.E., and Pines, A. (1988) A silicon-29 nuclear magnetic resonance study of silicon-aluminum ordering in leucite and analcime. *Physics and Chemistry of Minerals*, 15, 370–382.
- Palmer, D.C., Putnis, A., and Salje, E.K.H. (1988) Twinning in tetragonal leucite. *Physics and Chemistry of Minerals*, 16, 298–303.
- Palmer, D.C., Salje, E.K.H., and Schmahl, W.W. (1989) Phase transitions in leucite: X-ray diffraction studies. *Physics and Chemistry of Minerals*, 16, 714–719.
- Peacor, D.R. (1968) A high temperature single crystal diffractometer study of leucite, $(\text{K},\text{Na})\text{AlSi}_2\text{O}_6$. *Zeitschrift für Kristallographie*, 127, 213–224.
- Phillips, B.L., Kirkpatrick, R.J., and Putnis, A. (1989) Si,Al ordering in leucite by high-resolution ^{29}Al MAS NMR spectroscopy. *Physics and Chemistry of Minerals*, 16, 591–598.
- Robie, R.A., Hemingway, B.S., and Fisher, J.R. (1978) Thermodynamic properties of minerals and related substances at 298.15 K and 1 bar (10^5 Pascals) pressure and at higher temperatures. *U.S. Geological Survey Bulletin*, 1452, 456.
- Samoson, A. (1985) Satellite transition high-resolution NMR of quadrupolar nuclei in powders. *Chemical Physics Letters*, 119, 29–32.
- Taylor, D., and Henderson, C.M.B. (1968) The thermal expansion of the leucite group of minerals. *American Mineralogist*, 53, 1476–1489.
- Ulbrich, H.H., and Waldbaum, D.R. (1976) Structural and other contributions to the third-law entropies of silicates. *Geochimica et Cosmochimica Acta*, 40, 1–24.